

Supporting Information

Recovery of chlorophyll *a* derivative from *Spirulina maxima*, its purification and photosensitizing potential

Margarida Martins¹, Cristiana M. Albuquerque^{1,2}, Cátia F. Pereira^{1,2}, João A. P. Coutinho¹, M. Graça P. M. S. Neves², Diana C. G. A. Pinto², Maria Amparo F. Faustino²,
Sónia P. M. Ventura^{1*}

¹CICECO - Aveiro Institute of Materials, Chemistry Department, University of Aveiro, 3810-193 Aveiro, Portugal

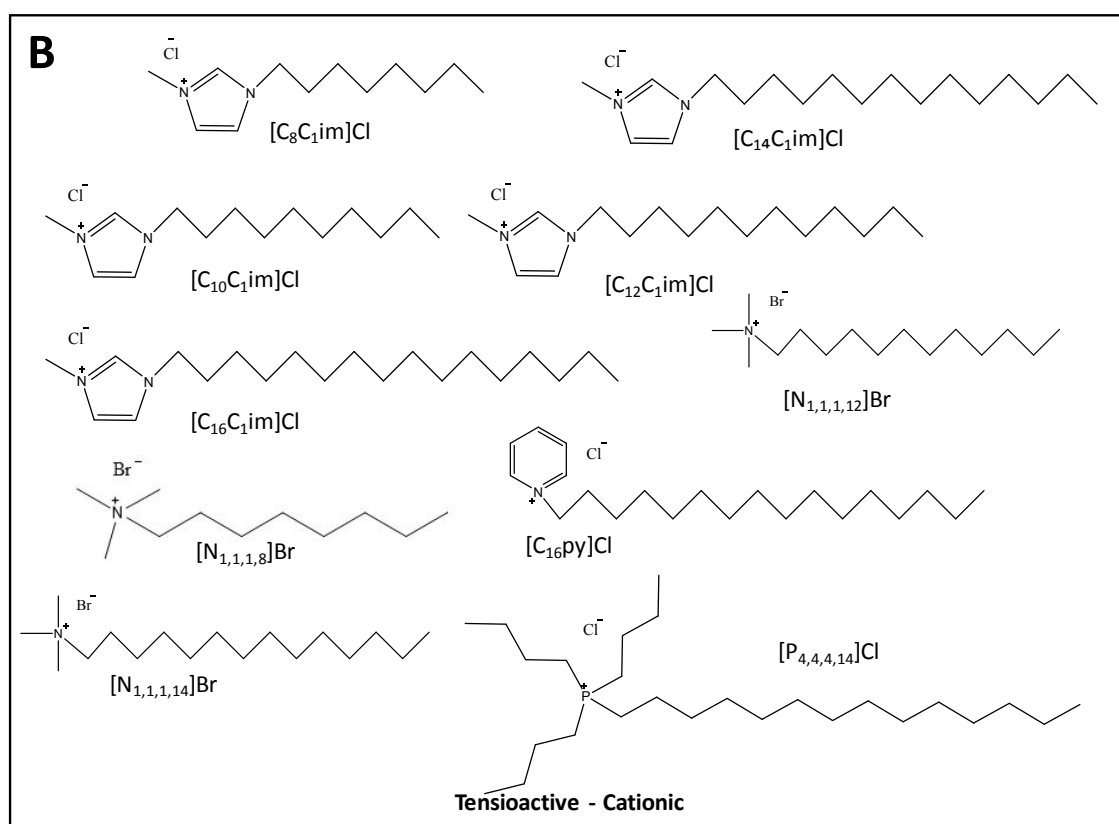
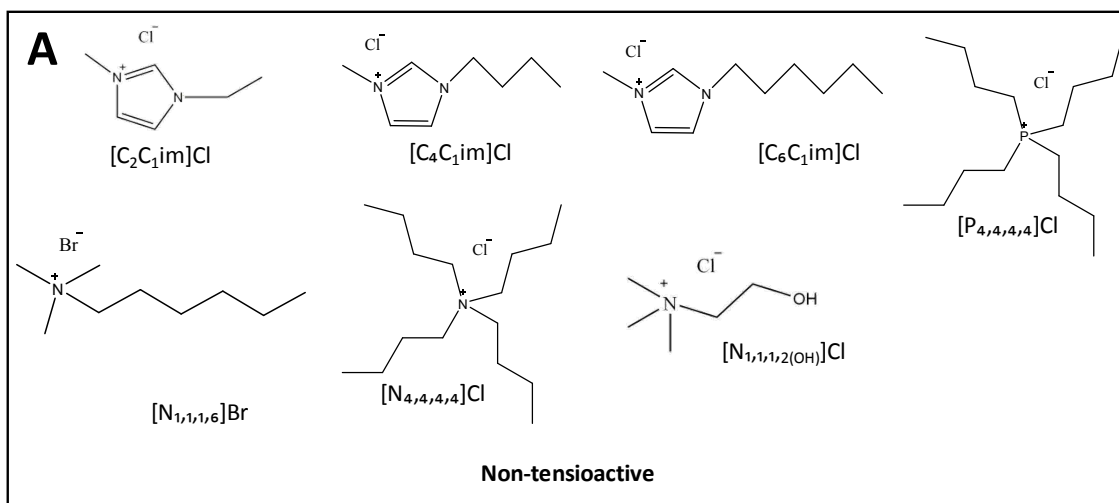
²LAQV - REQUIMTE, Department of Chemistry, University of Aveiro, 3810-193 Aveiro, Portugal

This document comprises: Pages: 11; Figures: 12; Tables: 2.

*Corresponding author:

Campus Universitário de Santiago. University of Aveiro. Aveiro. Portugal

Tel: +351-234-370200; Fax: +351-234-370084; E-mail address: spventura@ua.pt



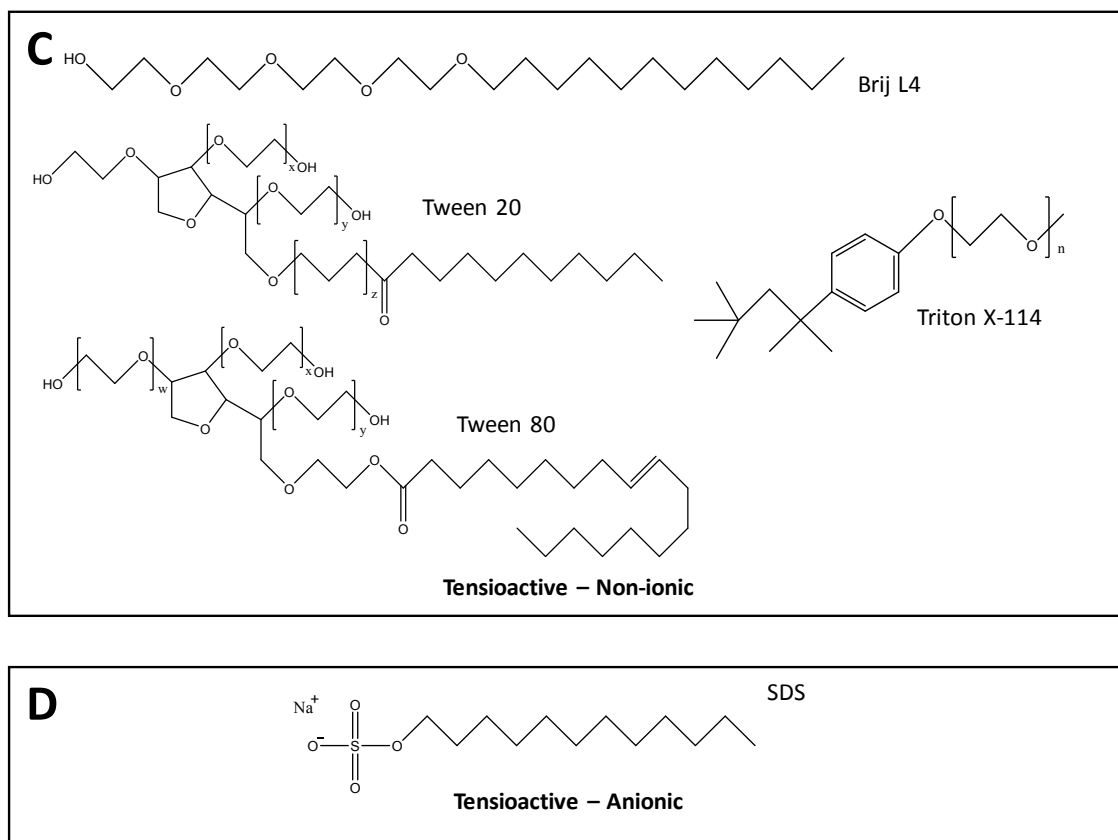


Figure S1. Molecular structure of the ILs and common surfactants screened in this work: (A) non-tensioactive compounds, (B) cationic tensioactive compounds, (C) non-ionic tensioactive compounds, and (D) anionic tensioactive compounds.

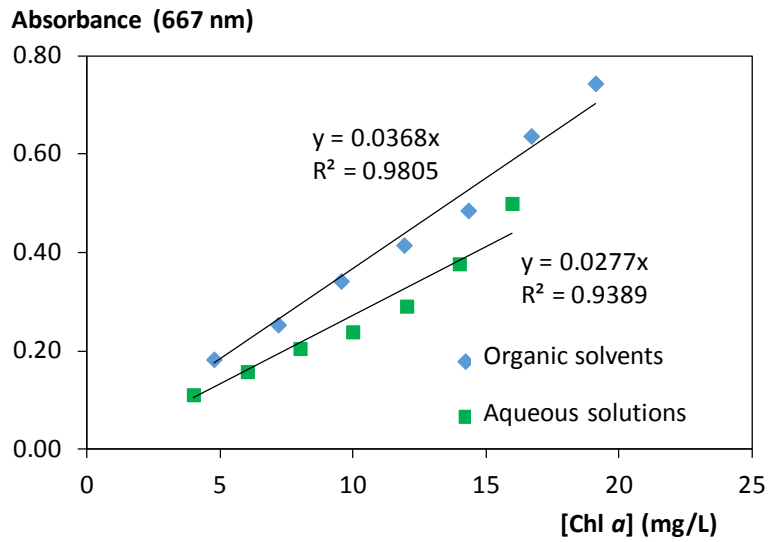


Figure S2. Calibration curves experimentally determined and used to quantify chlorophyll in organic solvents and aqueous solutions using the Synergy HT microplate reader – BioTek.

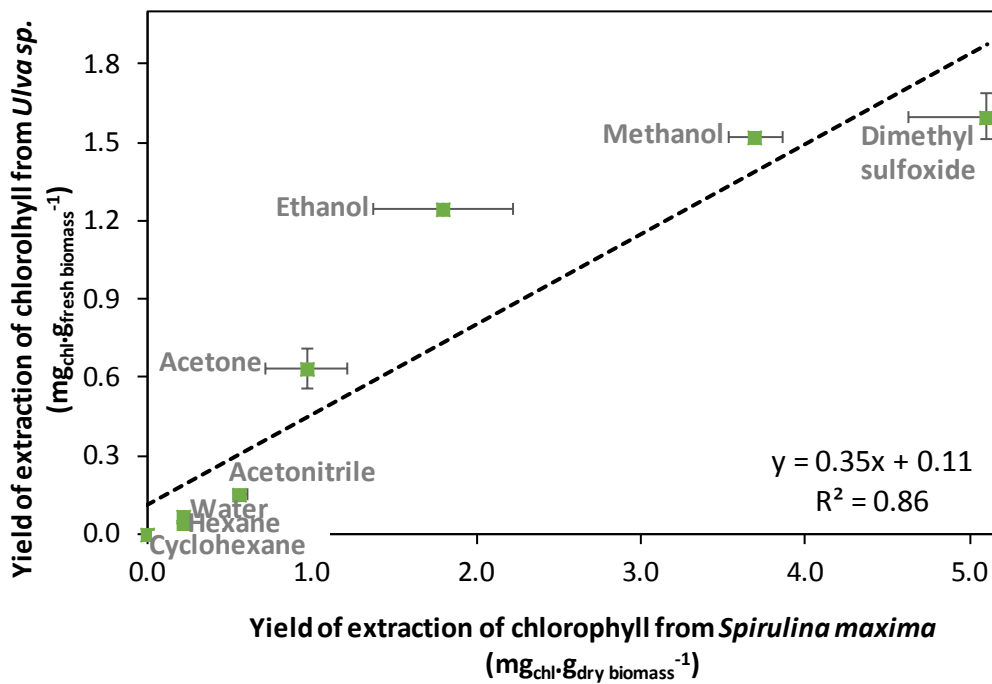


Figure S3. Correlation between the yields of chlorophyll extracted from *Ulva rigida*¹ and *Spirulina maxima* using the same solvents.

Table S1. Real and coded values of the optimization process expressed by the yields of chlorophyll extracted from *Spirulina maxima* by CCRD 2² using methanol as solvent.

Run	Design Matrix		Experimental conditions		Yield of extraction (mg _{chl} ·g _{dry biomass} ⁻¹)
	Time	Solid-liquid ratio	Time (min)	Solid-liquid ratio (g _{dry biomass} ·mL _{solvent} ⁻¹)	
1	-1	-1	28	0.030	2.698
2	1	-1	62	0.030	2.823
3	-1	1	28	0.055	1.837
4	1	1	62	0.055	2.287
5	-1.41	0	21	0.045	1.788
6	1.41	0	69	0.045	2.724
7	0	-1.41	45	0.024	3.052
8	0	1.41	45	0.059	1.869
9	0	0	45	0.045	2.350
10	0	0	45	0.045	2.731
11	0	0	45	0.045	2.510

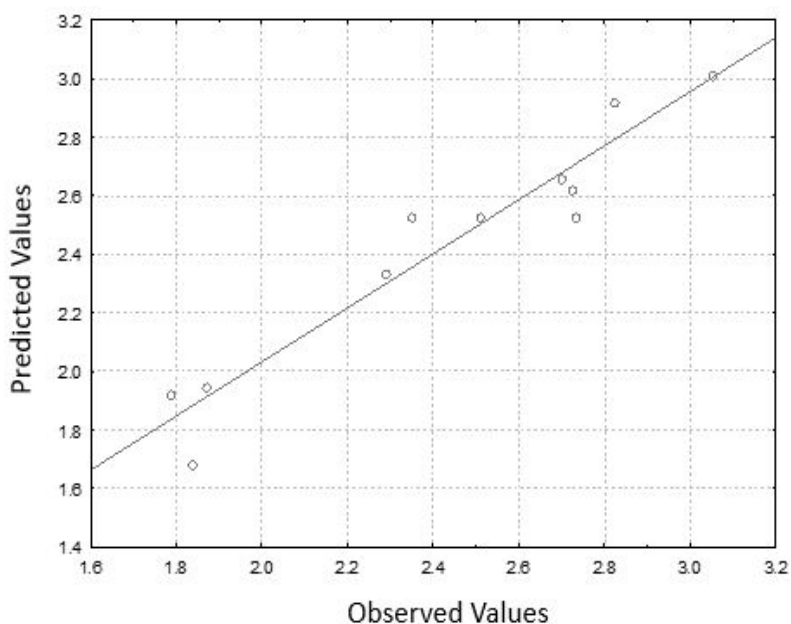


Figure S4. Predicted vs. experimental values of the CCRD (2²) regarding the yield of chlorophyll using methanol.

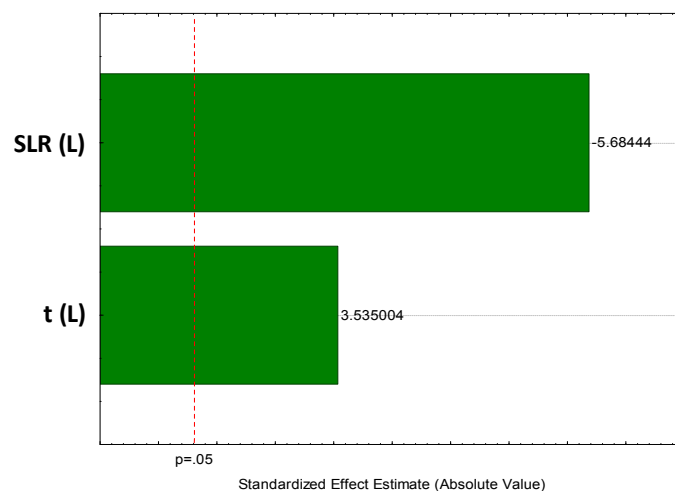


Figure S5. Pareto's chart of the CCRD regarding the yield of chlorophyll using methanol as solvent.

Table S2. Critical micellar concentration (CMC) values of the used tensioactive compounds.

Tensioactive compound	CMC (mM)	Reference
[C ₈ C ₁ im]Cl	220	2
[C ₁₀ C ₁ im]Cl	55	2
[C ₁₂ C ₁ im]Cl	15	2
[C ₁₄ C ₁ im]Cl	4	2
[C ₁₆ C ₁ im]Cl	1.26	3
[N _{1,1,1,8}]Cl	39.8	4
[N _{1,1,1,12}]Br	15.6	5
[N _{1,1,1,14}]Br	3.8	5
[C ₁₆ py]Cl	0.96	6
[P _{4,4,4,14}]Cl	4.69	4
SDS	8	2
Brij L4	n.d.	-
Triton X-114	0.168	7
Tween 20	0.050	7
Tween 80	0.010	7

RT: 0,00 - 38,00

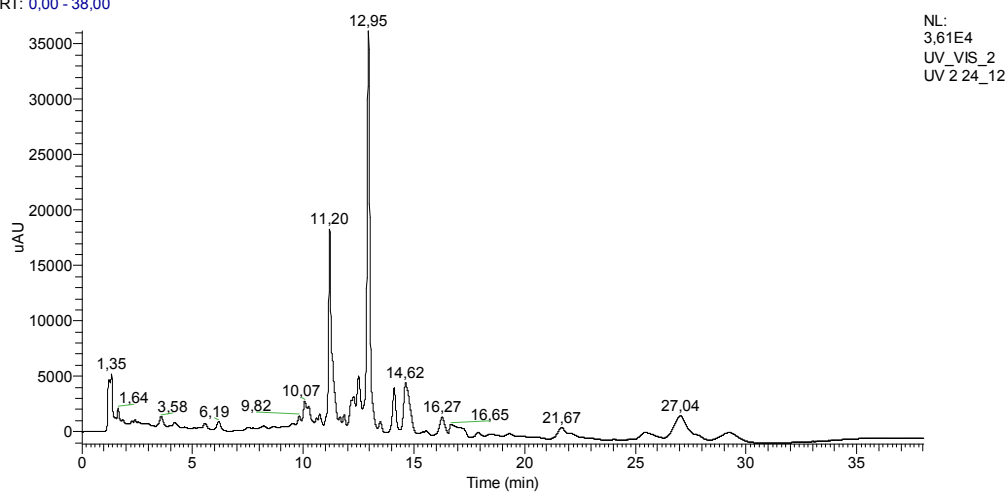


Figure S6. UHPLC chromatogram of the methanol-based extract, recorded at 305 nm.

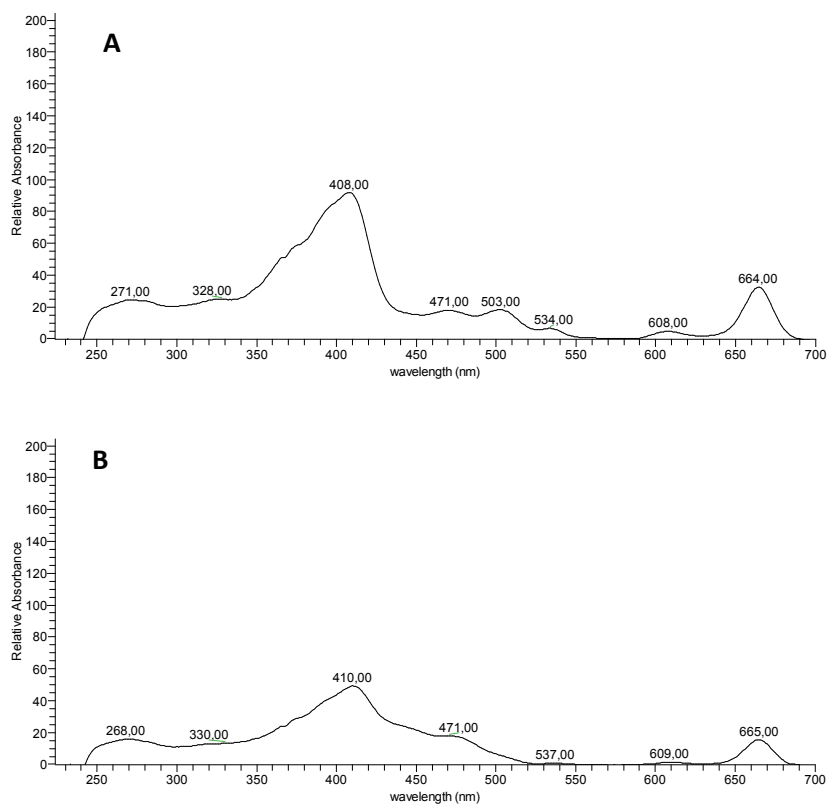


Figure S7. UV-Vis spectra of the methanol-based extract considering the peaks at (A) 11.20 min and (B) 12.95 min.

RT: 0,00 - 37,99

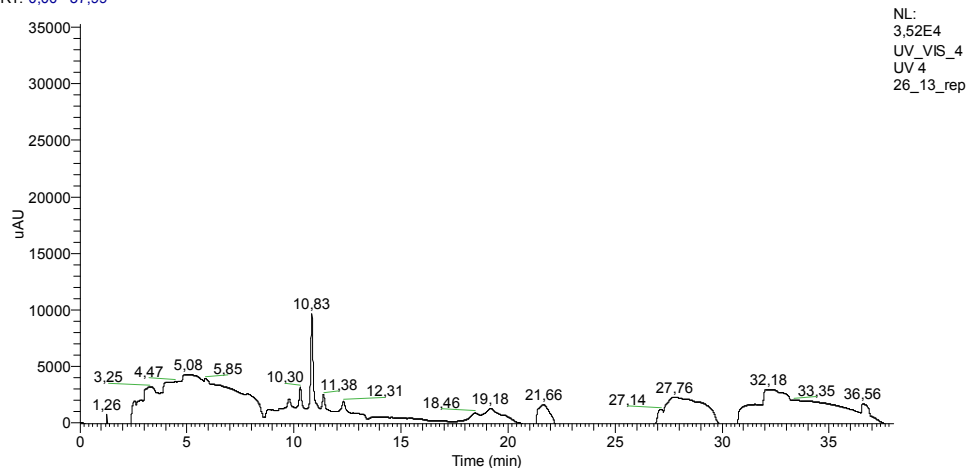


Figure S8. UHPLC chromatogram of the 1st and 2nd fractions of back extraction (obtained from alternative extraction), recorded at 430 nm.

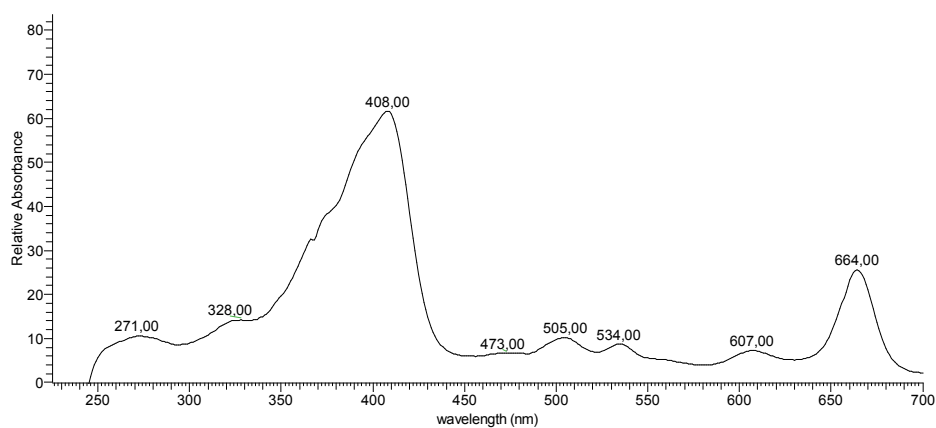


Figure S9. UV-Vis spectra of the 1st and 2nd fractions of back extraction (obtained from alternative extraction) considering the peak at 10.83 min.

RT: 0,00 - 37,99

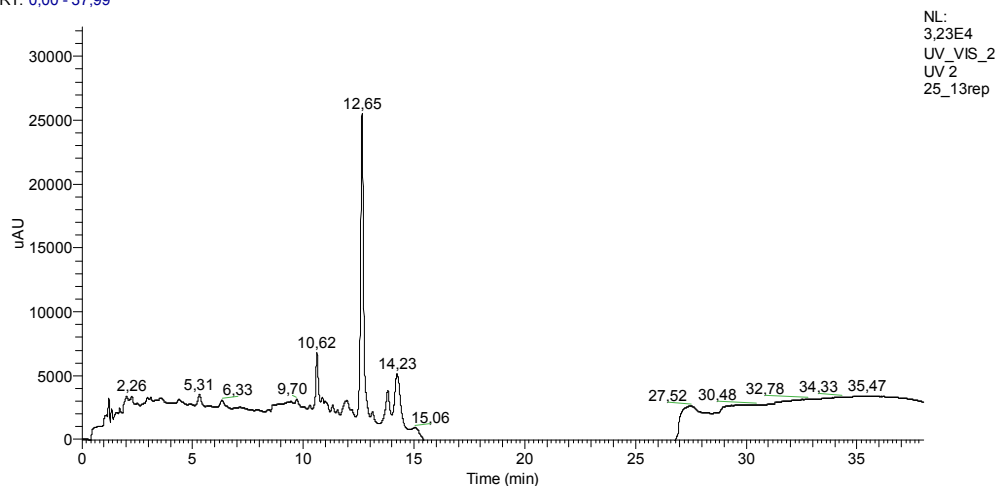


Figure S10. UHPLC chromatogram of the 3rd fraction of back extraction (obtained from alternative extraction), recorded at 305 nm.

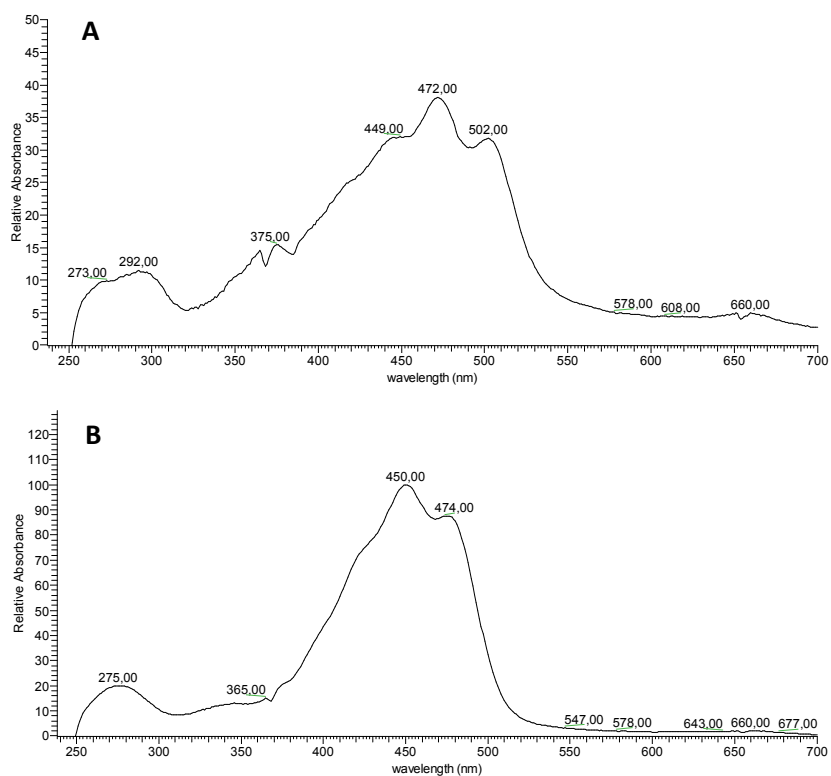


Figure S11. UV-Vis spectra of the 3rd fraction of back extraction (obtained from alternative extraction) considering the peaks at (A) 10.62 min and (B) 12.65 min.

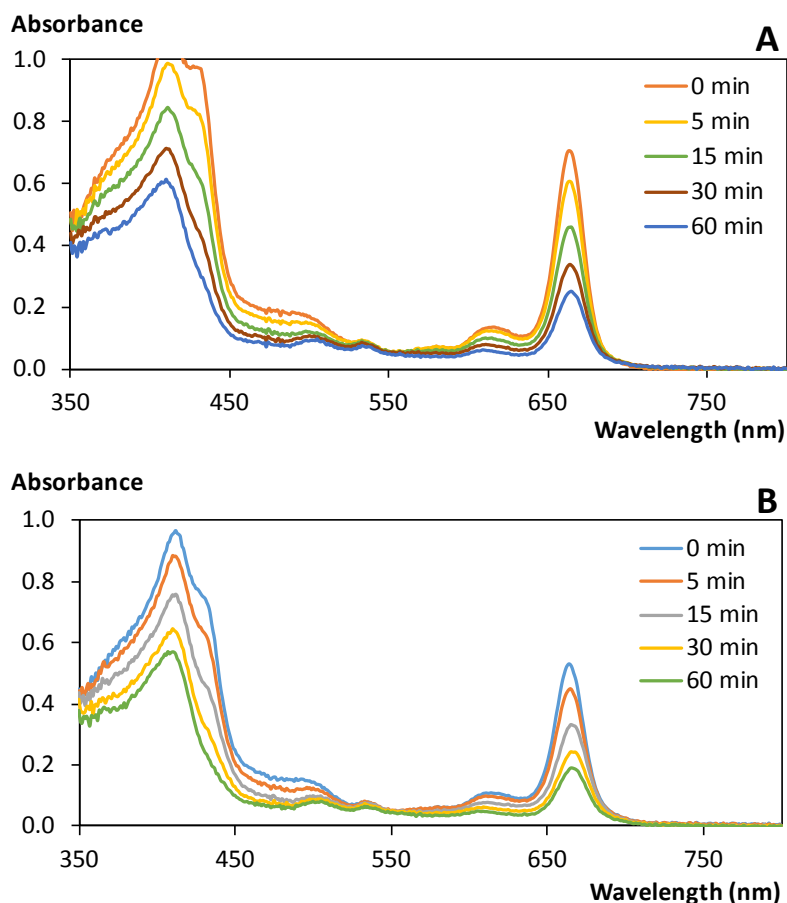


Figure S12. UV-Vis spectra of the (A) methanol-based extract and (B) 1st and 2nd fractions of back extraction (obtained from alternative extraction) along the irradiation period in the photostability assays.

References

- (1) Martins, M.; Oliveira, R.; Coutinho, J. A. P.; Faustino, M. A. F.; Neves, M. G. P. M. S.; Pinto, D. C. G. A.; Sónia, P. M. Recovery of pigments from *Ulva rigida*. *Sep. Purif. Technol.* **2020**, DOI: 10.1016/j.seppur.2020.117723.
- (2) Blesic, M.; Marques, M. H.; Plechkova, N. V; Seddon, K. R.; Rebelo, L. P. N.; Lopes, A. Self-aggregation of ionic liquids: micelle formation in aqueous solution. *Green Chem.* **2007**, 9 (5), 481–490, DOI: 10.1039/B615406A

- (3) Jungnickel, C.; Łuczak, J.; Ranke, J.; Fernández, J. F.; Müller, A.; Thöming, J. Micelle formation of imidazolium ionic liquids in aqueous solution. *Colloids Surfaces A Physicochem. Eng. Asp.* **2008**, *316*, 278–284, DOI: 10.1016/j.colsurfa.2007.09.020
- (4) Vicente, F. A.; Cardoso, I. S.; Sintra, T. E.; Marques, E. F.; Ventura, S. P. M.; Coutinho, J. A. P. The impact of surface active ionic liquids on the cloud points of nonionic surfactants and the formation of aqueous micellar two-phase systems. *J. Phys. Chem. B* **2017**, *121* (37), 8742–8755, DOI: 10.1021/acs.jpccb.7b02972
- (5) Garcia-Mateos, I.; Mercedes Velázquez, M.; Rodriguez, L. J. Critical micelle concentration determination in binary mixtures of ionic surfactants by deconvolution of conductivity/concentration curves. *Langmuir* **1990**, *6*, 1078–1083, DOI: 10.1021/la00096a009
- (6) Chatterjee, A.; Moulik, S. P.; Sanyal, S. K.; Mishra, B. K.; Puri, P. M. Thermodynamics of micelle formation of ionic surfactants: A critical assessment for sodium dodecyl sulfate, cetyl pyridinium chloride and dioctyl sulfosuccinate (Na Salt) by microcalorimetric, conductometric, and tensiometric measurements. *J. Phys. Chem. B* **2001**, *105* (51), 12823–12831, DOI: 10.1021/jp0123029
- (7) Hait, S. K.; Moulik, S. P. Determination of critical micelle concentration (CMC) of nonionic surfactants by donor-acceptor interaction with iodine and correlation of CMC with hydrophile-lipophile balance and other parameters of the surfactants. *J. Surfactants Deterg.* **2001**, *4* (3), 303–309, DOI: 10.1007/s11743-001-0184-2